THE JOURNAL OF BIOLOGICAL CHEMISTRY
Vol. 278, No. 15, Issue of April 11, pp. 13462–13467, 2003
Printed in U.S.A.

Homotetrameric Structure of the SNAP-23 N-terminal Coiled-coil Domain*

Received for publication, October 13, 2002, and in revised form, December 23, 2002
Published, JBC Papers in Press, January 29, 2003, DOI 10.1074/jbc.M210483200

Steven J. Freedman‡§¶, Hyun Kyu Song§‖, Yingwu Xu§‖, Zhen-Yu J. Sun‖, and Michael J. Eck§‖

From the ‡Division of Hemostasis and Thrombosis, Beth Israel Deaconess Medical Center, Boston, Massachusetts 02115, the ‖Department of Biological Chemistry and Molecular Pharmacology, Harvard Medical School, Boston, Massachusetts 02115, and the §Department of Cancer Biology, Dana-Farber Cancer Institute, Boston, Massachusetts 02115

SNARE proteins mediate intracellular membrane fusion by forming a coiled-coil complex to merge opposing membranes. A "fusion-active" neuronal SNARE complex is a parallel four-helix bundle containing two coiled-coil domains from SNAP-25 and one coiled-coil domain each from syntaxin-1a and VAMP-2. "Prefusion" assembly intermediate complexes can also form from these SNAREs. We studied the N-terminal coiled-coil domain of SNAP-23 (SNAP-23N), a non-neuronal homologue of SNAP-25, and its interaction with other coiled-coil domains. SNAP-23N can assemble spontaneously with the coiled-coil domains from SNAP-23C, syntaxin-4, and VAMP-3 to form a heterotetrameric complex. Unexpectedly, pure SNAP-23N crystallizes as a coiled-coil homotetrameric complex. The four helices have a parallel orientation and are symmetrical about the long axis. The complex is stabilized through the interaction of conserved hydrophobic residues comprising the *a* and *d* positions of the coiled-coil heptad repeats. In addition, a central, highly conserved glutamine residue (Gln-48) is buried within the interface by hydrogen bonding between glutamine side chains derived from adjacent subunits and to solvent molecules. A comparison of the SNAP-23N structure to other SNARE complex structures reveals how a simple coiled-coil motif can form diverse SNARE complexes.

Endosomal trafficking and vesicle secretion in eukaryotic cells requires fusion of membrane compartments. Synaptic vesicle secretion in neurons has served as a paradigm for understanding the molecular basis for membrane fusion (1). In general, a v-SNARE[1] called VAMP (synaptobrevin) is associated with the vesicle membrane and two t-SNAREs called SNAP-25 and syntaxin are associated with the plasma or target membrane. According to the SNARE hypothesis, specific pairing between v- and t-SNAREs brings together two membranes for fusion (2). Following fusion, NSF and SNAPs dissociate the SNARE complex in an ATP-dependent reaction (3).

SNARE proteins contain coiled-coil regions that mediate complex formation (4). VAMP and syntaxin proteins each have a single SNARE-interacting coiled-coil domain followed by a C-terminal transmembrane domain, whereas SNAP-25 proteins have N- and C-terminal coiled-coil domains separated by a loop that attaches to membranes via palmitoylated cysteines (5). The coiled-coil sequences are highly conserved among SNARE families (4). The homologous regions are made up of ~8 heptad repeats in which the hydrophobic residues in the *a* and *d* positions of each repeat align in 16 layers (4). The central "0" layer is uniquely polar and consists of a glutamine in syntaxin and the SNAP-25 N- and C-terminal coiled-coil domains and an arginine in the VAMP coiled-coil domain. The structure of a core SNARE complex from neurons revealed a parallel four-helix bundle composed of two coiled-coil domains from SNAP-25, and one coiled-coil domain each from syntaxin-1a and VAMP-2 (6, 7). The parallel orientation of SNARE proteins attached to opposite membranes suggests a "zipper-like" mechanism for membrane fusion (7). A distantly related endosomal SNARE complex has a very similar structure, suggesting a common fusion mechanism mediated by neuronal, endosomal, and possibly other SNARE complexes (8).

SNARE isoforms SNAP-23, syntaxin-4, and VAMP-3 (Cellubrevin) are present in many non-neuronal cell types (9–12). Foster *et al.* (13) found that soluble forms of SNAP-23, syntaxin-4, and VAMP-2 (present in neurons and other cells) formed binary complexes but not a native-like ternary complex. In contrast, Yang *et al.* (14) found that the coiled-coil domains of these proteins could form a heterotetrameric complex. However, the stability of this non-neuronal SNARE complex was decreased relative to a neuronal one composed of SNAP-25, syntaxin-1a, and VAMP-2. These studies suggest that this group of non-neuronal SNARE proteins may function differently than the neuronal ones.

The structures of non-neuronal SNAREs and their complexes are not well characterized. We used a structural approach to understand the function of non-neuronal SNARE proteins involved in membrane fusion. Interestingly, we find that SNAP-23N (Fig. 1) can form a parallel four-helix bundle in the absence of other SNARE proteins. The 2.3-Å crystal structure of SNAP-23N reveals important similarities and differences with other SNARE complex structures. Comparison of these structures extends our understanding of how SNARE proteins assemble and function.

* The costs of publication of this article were defrayed in part by the payment of page charges. This article must therefore be hereby marked "*advertisement*" in accordance with 18 U.S.C. Section 1734 solely to indicate this fact.

The atomic coordinates and structure factors (code 1NHL) have been deposited in the Protein Data Bank, Research Collaboratory for Structural Bioinformatics, Rutgers University, New Brunswick, NJ (http://www.rcsb.org/).

¶ Supported by a National Institutes of Health (NIH) K08 award from the NHLBI, NIH and an ASH Scholar Award from the American Society of Hematology. To whom correspondence should be addressed: Division of Hemostasis and Thrombosis, Beth Israel Deaconess Medical Center, 41 Avenue Louis Pasteur, Boston, MA 02115. Tel.: 617-667-0719; Fax: 617-667-2030; E-mail: sfreedm2@caregroup.harvard.edu.

[1] The abbreviations used are: SNARE, SNAP receptor; SNAP, soluble NSF attachment protein; NSF, *N*-ethylmaleimide-sensitive fusion protein; v-SNARE, vesicle SNARE; t-SNARE, target SNARE; SNAP-25, synaptosome-associated protein of 25 kDa; SNAP-23, SNAP-25-like protein of 23 kDa; VAMP, vesicle-associated membrane protein; MAD, multiwavelength anomalous diffraction; SeMet, selenomethionine; GST, glutathione *S*-transferase; MALDI-TOF, matrix-assisted laser desorption ionization time-of-flight.

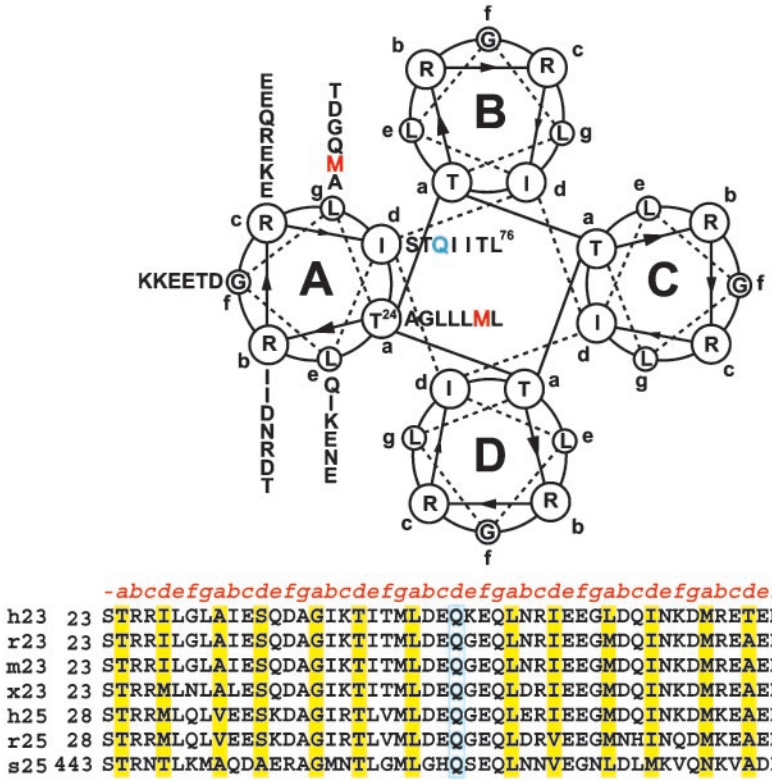

FIG. 1. **Helical wheel diagram of the SNAP-23N homotetramer showing residues 24–76.** View is from the N terminus, and residues in the first two helical turns are *circled*. Heptad positions are labeled *a* through *g*. Note that residues that make intermolecular contacts are located in heptad positions *a* and *d* and make 16 intermolecular planes or "layers." A central highly conserved glutamine residue is highlighted in *blue*, and the two methionines derivatized with selenium for crystallographic phasing are highlighted in *red*. Below, alignment of SNAP-23N and SNAP-25N sequences is shown. Conserved heptad repeat *a* and *d* residues are highlighted in *yellow*, and the central conserved glutamine is highlighted in *blue*. The aligned sequences are: *h*, *Homo sapiens*; *r*, *Rattus norvegicus*; *m*, *Mus musculus*; *x*, *Xenopus laevis*; *s*, *Sachharomyces cervesiae* (SNAP-25 yeast homologue called sec9). The *top* figure was adapted from Harbury *et al.* (27).

EXPERIMENTAL PROCEDURES

Protein Expression and Purification—PCR DNA fragments encoding amino acids 19–71 of rat VAMP-3 (100% identical to human), 210–262 of rat syntaxin-4 (94% identical to human), and 23–76 and 156–208 of human SNAP-23 were cloned into the *Bam*HI and *Eco*RI sites of a pET vector (Novagen) that expresses glutathione *S*-transferase (GST) fusion proteins containing a thrombin protease site. The expression plasmid introduces a vector-derived Gly-Ser at the N terminus of each peptide that remains after thrombin cleavage. The constructs were transformed individually into BL21 (DE3) *Escherichia coli* cells. To prepare selenomethionine-substituted SNAP-23N (SeMet-SNAP-23N), the SNAP-23N-expressing plasmid was transformed into B834 (DE3) methionine auxotroph *E. coli* cells and grown in M9 minimal medium containing a complete complement of amino acids except for methionine substituted by selenomethionine (Sigma). Bacteria were grown in 50 μg/ml ampicillin, and expression was induced with isopropyl-1-thio-β-D-galactopyranoside for 3 h at 37 °C beginning at OD_{600} = 0.5–0.6. Bacteria were lysed by sonication in 50 mM Tris-HCl, pH 7.5, 100 mM NaCl, and one complete protease inhibitor tablet (Roche Molecular Biochemicals), and the peptides in the supernatant fraction were isolated over glutathione-Sepharose 4B resin (Amersham Biosciences). The peptides were eluted with thrombin protease and further purified over a Superdex 75 gel filtration column equilibrated in 50 mM Tris-HCl, pH 7.5, and 100 mM NaCl using an ÄKTApurifier (Amersham Biosciences). SNAP-23C is poorly soluble after concentration, but an adequate amount for the binding assay (see "Results") could be achieved by directly using the SNAP-23C eluate from purifed GST-SNAP-23C attached to glutathione beads. Peptides were concentrated over YM-3 microcon membranes (Millipore), and their final concentrations were determined using the Coomassie plus protein assay reagent (Pierce) with bovine serum albumin as a standard. Purity was determined by SDS-PAGE and MALDI-TOF mass spectroscopy.

SNARE Binding Assay—Approximately equimolar amounts (20 μM) of VAMP-3, syntaxin-4, SNAP-23N, and SNAP-23C coiled-coil peptides were mixed together in the indicated combinations and incubated at 4 °C for 2 h. The binding buffer contained 50 mM Tris-HCl, pH 7.5, and 50 mM NaCl. Aliquots of each binding reaction were analyzed by nondenaturing electrophoresis on 10% polyacrylamide gels.

Crystallization, X-ray Diffraction Data Collection, and Phasing—Underivatized SNAP-23N was crystallized by the hanging drop vapor diffusion method at 23 °C. SNAP-23N was crystallized at a concentration of 1–4 mg/ml by combining 1 μl of purified protein in 50 mM Tris-HCl, pH 7.5, 100 mM NaCl with 1 μl of reservoir solution containing 0.1 M Hepes, pH 7.5, 0.2 M $CaCl_2$, and 28% polyethylene glycol (PEG) 400. Typically, crystals were observed within 24 h and grew to maximal size by 48–72 h. SeMet-SNAP-23N was crystallized using the same buffer conditions, but at 4 °C.

Diffraction data were collected by flash-freezing crystals from the mother liquor in the cryostream at 100 K. Native diffraction data were recorded on a 300 mm MarResearch image plate detector using a rotating anode source with mirror optics (Osmic™). Multiwavelength anomalous diffraction (MAD) data were recorded on a Brandeis four-module CCD detector at beamline X-12C of the National Synchrotron Light Source of Brookhaven National Laboratories. Data were processed and scaled using DENZO/SCALEPACK (15) for home data and HKL2000 (15) for MAD data. Native crystals diffracted x-rays on the home detector to 2.5-Å resolution and SeMet crystals diffracted at the synchrotron source to 2.3 Å resolution. Crystallographic data are summarized in Table I.

Structure Determination—Molecular replacement with COMO (16) using the coordinates for rat SNAP-25N (7) as a search model yielded clear rotation and translation solutions for the peptide. The resulting $2F_o - F_c$ electron density map was readily interpretable for the N-terminal region of SNAP-23N, but weak density for the more C-terminal region of the structure complicated rebuilding and refinement. Therefore, we recorded a three-wavelength MAD data set with SeMet-substituted peptide. An electron density map generated from the MAD data confirmed the molecular replacement solution and revealed clear density for most of the peptide sequence. However, density for the C-terminal 8 residues was relatively weak. The selenium positions of the 2 SeMet residues were located and refined with SOLVE (17) using data from 20 to 3 Å. Manual rebuilding with O (18) and refinement with CNS (19) to the higher resolution SeMet data produced a final model with an R value of 27.3% and a free R value of 31.6%. The higher than expected final R factor may be a consequence of the relatively weak density and high thermal parameters for the C-terminal 8 residues in the structure. Similar R factors were reported for a related SNARE complex for similar reasons (20). The final model contains residues 23–76 of SNAP-23N and 43 solvent molecules.

RESULTS

Non-neuronal SNARE peptides from SNAP-23, syntaxin-4, and VAMP-3 were expressed recombinantly in bacteria and purified as described under "Experimental Procedures." The N- and C-terminal boundaries were chosen based on homology to

TABLE I
Crystallographic data

Data collection statistics				
Data set	Native		SeMet	
Space group	$P42_12$		$P42_12$	
a (Å)	34.43		34.91	
c (Å)	81.51		81.69	
Resolution range (Å)	50–2.5		50–2.3	
		L1	L2	L3
Wavelength (Å)	1.5418	0.9788 (f′ min)	0.9785 (f′ max)	0.9500
Unique reflections	1801	2385	2381	2407
Completeness (%)	91.7	92.8	92.8	94.8
R_{merge} [a]	0.044	0.055	0.060	0.055
Refinement and model statistics[b]				
FOM (MAD/density modified)[c]	0.64/0.72			
R-factor/*R*-free (%)[d]	27.3/31.6			
Resolution range (Å)[e]	20–2.3			
Average *B*-factors (Å^2)				
Main chain	29.1			
Side chain	32.7			
Solvent	41.3			
r.m.s.d. from ideality[f]				
Bonds (Å)	0.005			
Angles (°)	1.00			

[a] $R_{merge} = \Sigma \mid I_{obs} - I_{ave} \mid / \Sigma I_{ave}$.
[b] Based on MAD data.
[c] FOM, figure of merit $((\cos\varphi)^2 + (\sin\varphi)^2)^{1/2}$; 20–3 Å.
[d] *R*-factor = $\mid F_{obs} - F_{calc} \mid / \Sigma \mid F_{obs} \mid$, where free *R* is calculated for 10% of reflections.
[e] No data cutoff.
[f] r.m.s.d., root mean square deviation.

the coiled-coil regions in the neuronal SNARE complex (4). Each peptide is a 55-mer (including the vector-derived N-terminal Gly-Ser) that correponds to 7.5 heptad repeats. All peptides except the SNAP-23C peptide were soluble in the millimolar range in aqueous solution; SNAP-23C has a pI of 9.39, which may contribute to its modest solubility. A binding assay using native polyacrylamide gel electrophoresis was performed to determine whether the SNARE peptides could interact with each other. Mixing equimolar amounts of all four peptides yielded a new complex band not observed with any of the three-way combinations of peptides (Fig. 2*A*). In another binding experiment, GST-SNAP-23C attached to glutathione beads was mixed with the other three SNARE peptides, and a pure peptide complex was eluted by thrombin cleavage. This purified complex had similar electrophoretic mobility on a native gel (Fig. 2*B*) and contained the coiled-coil domains of four SNARE peptides as verified by MALDI-TOF mass spectroscopy. We conclude that the coiled-coil domains from SNAP-23, syntaxin-4, and VAMP-3 can form a heterotetrameric complex. To date, we have been unable to obtain crystals of this heterotetramer, in part due to the poor solubility of SNAP-23C, which has prevented preparation of large quantities of the complex. However, we did observe small crystals in an initial screen in which equimolar amounts of SNAP-23N, SNAP-23C, syntaxin-4, and VAMP-3 were combined. Surprisingly, analysis of these crystals by mass spectroscopy demonstrated that they contained only SNAP-23N. It is likely that rapid precipitation of SNAP-23C, and possibly other SNARE peptides, in this experiment prevented formation of the expected heterotetramer. Subsequently, we determined the SNAP-23N structure to provide insight into its quaternary structure and potential function. The human SNAP-23N sequence is shown aligned with homologous sequences in Fig. 1.

Purified SNAP-23N crystallized in the presence of divalent metal ions (*e.g.* $CaCl_2$ or $MgCl_2$). The native crystals are rectangular prisms with approximate dimensions of $0.08 \times 0.02 \times 0.02$ mm^3, whereas the SeMet crystals are square plates with approximate dimensions of $0.13 \times 0.13 \times 0.01$ mm^3. Both crystal forms have the same tetragonal space group with one copy of SNAP-23N in the asymmetric unit. Symmetry constraints resulting from the 4-fold symmetry of the space group suggested that SNAP-23N molecules were organized as a parallel homotetrameric complex. Structure determination confirmed this prediction (see below).

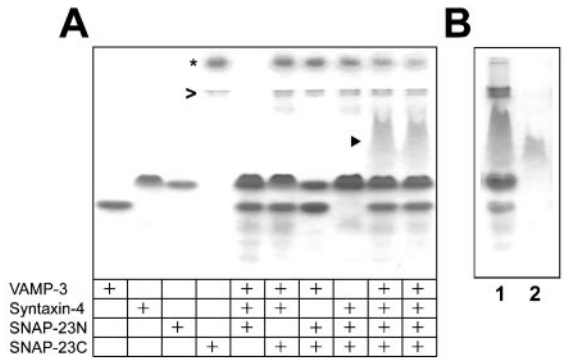

FIG. 2. **SNARE peptide binding assay.** *A*, individual SNARE peptides (*first four lanes*) and mixtures of SNARE peptides (*last six lanes*) are shown on a non-denaturing polyacrylamide gel. The *last two lanes* are a duplicate experiment of all four peptides mixed together. The SNAP-23C peptide (*asterisk*) migrates poorly due to its high pI (9.39), and the weaker band beneath it is contaminating GST (*open arrow*). Coomassie-stained protein bands other than the individual forms represent heterodimeric and heterotrimeric complexes of SNARE peptides as reported by others (22). Note that the *last two lanes* contain a new, slowly migrating "diffuse" band (*closed arrow*) that is not present in lanes containing three-way combinations of peptides. These bands represent the putative SNARE peptide heterotetramer. *B*, purification of the SNARE peptide heterotetramer (*lane 2*) from a mixture of purified SNAP-23N, SNAP-23C, syntaxin-4, and GST-SNAP-23C (*lane 1*). The composition of this pure band containing all four peptides was determined by mass spectroscopy (see "Results" for details).

Each SNAP-23N molecule is an extended amphipathic α helix with 14 helical turns. The left-handed superhelical twist of the complex results in a ~13° bend in each helix (Fig. 4*A*). The electron density map shows excellent main chain connectivity along its entire length from Ser-23 to Leu-76 (Fig. 3). However, the side chain conformations of surface-exposed residues between Lys-64 and Leu-81 are less well defined. Four molecules of SNAP-23N produce a parallel four-helix bundle

with overall dimensions of ~80 × 24 × 24 Å^3 (Fig. 4, *A* and *B*). Each peptide in the complex has the same conformation, and thus, the tetramer has exact 4-fold symmetry as required by the tetragonal crystal lattice. The SNAP-23N peptide is acidic (pI = 4.70), and the complex displays a mostly electronegative solvent-exposed surface; in contrast, the complex interface is mostly neutral (Fig. 4*C*).

The homotetrameric complex is held together primarily through hydrophobic interactions (Fig. 5*A*). Hydrophobic residues occupy the *a* and *d* positions of the coiled-coil heptad repeats, and their side chains face the interior of the complex (Fig. 1). The only exception is Gln-48 whose polar side chain is also buried in the interface (Fig. 5*B*). Thus, planes of buried residues occur at regular intervals along the chain and create 16 layers of intermolecular contacts. Gln-48 is located in the central or 0 layer as in other SNARE complexes. Our structure shows that the polar groups of the Gln-48 side chains point toward the center of the complex and are only 2.5 Å apart from one another (Fig. 5*B*). Although it is a deviation from the strict crystallographic symmetry, we have modeled the four Gln-48 residues with alternating side chain rotamers as it allows chemically reasonable hydrogen bonding in the tetramer. In addition, a water molecule hydrogen bonds to the free polar group not coordinated by a Gln-48 side chain in an adjacent molecule (Fig. 5*B*).

Although Ca^{2+} is required for secretion in a variety of cell types (21) and divalent cations were required for crystallization, Ca^{2+} ions were not observed in the electron density map in the crystal structure. Thus, Ca^{2+} ions may have a nonspecific stabilizing effect on the SNARE complex structure.

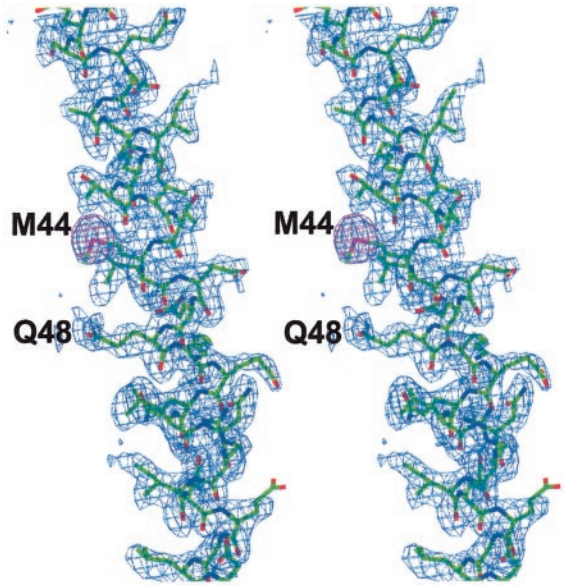

FIG. 3. **Electron density map of the SNAP-23N structure.** A region of a single SNAP-23N peptide (Glu-33 to Leu-59) of the asymmetric unit is shown fitted to the electron density map derived from experimental MAD data. The electron density map (*cyan*) was contoured using a 1σ cutoff. The anomalous difference map (*violet*) contoured at 7σ shows the position of selenium in SeMet-44. Gln-48 is labeled for orientation. This figure was prepared with the program CHAIN (32).

DISCUSSION

We found that SNAP-23N can associate with other nonneuronal SNARE coiled-coil domains to form a minimum heterotetrameric complex. This result is in agreement with the findings of Yang *et al.* (14) who used coiled-coil domains from SNAP-23, syntaxin-4, and VAMP-2 (98% identical to VAMP-3) but conflicts with the work of Foster *et al.* (13) who could not detect a ternary complex using GST-fused cytoplasmic regions of the same proteins. It is possible that the assay conditions of the latter study were not suitable for creating a ternary complex.

Work by others (22, 23) indicated that the neuronal SNAP-23N homologue, SNAP-25N, is mostly unstructured in solution. SNAP-23N and SNAP-25N are 72% identical and so might be expected to behave similarly. On the other hand, heterotetrameric coiled-coil complexes containing SNAP-25 have a higher stability compared with those containing SNAP-23 (14); perhaps the driving force for SNAP-23N self-association destabilizes its interaction with other SNARE coiled-coil domains.

Comparison of the SNAP-23N structure to other SNARE complexes reveals important similarities and differences. Like the SNAP-23N homotetramer, the neuronal heterotetramer and complexes between the SNAP-25 coiled-coil domains with the syntaxin-1a coiled-coil domain are arranged as parallel four-helix bundles (7, 23–25). In contrast, a syntaxin-1a homotetramer contains two pairs of helices that run antiparallel to one another (26). The neuronal heterotetrameric complex has a much larger left-handed helical twist compared with the SNAP-23N homotetramer, because each chain in the heterotetramer has a slightly different conformation. Despite these differences the SNAP-23N homotetramer and neuronal heterotetramer appear remarkably similar (Fig. 6*B*). In fact, superimposition of the SNAP-23N and SNAP-25N chains re-

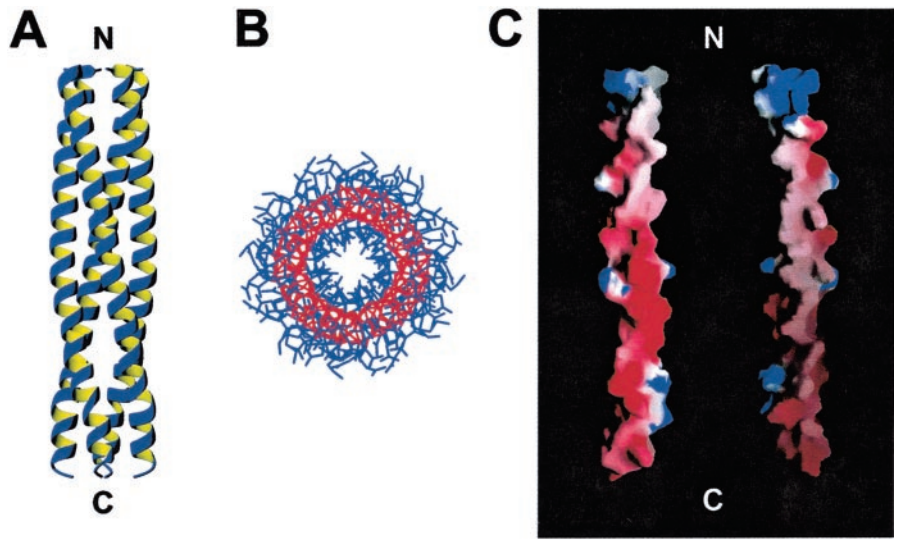

FIG. 4. **Structure of SNAP-23N.** *A*, SNAP-23N is a parallel homotetramer with perfect 4-fold symmetry. It is shown down its long axis, demonstrating that the chains wrap around each other to produce a left-handed superhelical twist. *B*, the SNAP-23N tetramer is shown end-on. The backbone is colored *red*, and the side chains are colored *blue*. Within the center of the tetramer are the side chains of the *a* and *d* residues of the heptad repeats that make intermolecular contacts. *C*, electrostatic surface of one SNAP-23N molecule. The solvent exposed surface (*left*) is mostly acidic (*red*), whereas the buried surface (*right*) is mostly hydrophobic or neutral charged (*white*). *A* and *B* were prepared with the program MolMol (33) and *C* with the program GRASP (34).

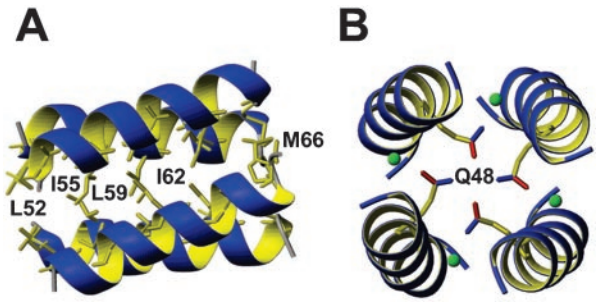

FIG. 5. **Intermolecular contacts in the SNAP-23N homotetramer.** *A*, intermolecular hydrophobic contacts are shown in the helical stretch from residues 51–67. The buried hydrophobic residues occupy heptad repeat positions *a* and *d*. *B*, Gln-48 is buried in the center of the complex within the 0 layer. The helical stretch from residues 40–56 is displayed as a *ribbon*. The side chain carbonyl (*red*) and amide (*blue*) groups from alternating molecules hydrogen bond with each other. A water molecule (*green*) hydrogen bonds to the "free" polar group of each monomer. All hydrogen bonds are ~2.5 Å apart. This figure was prepared with the program MolMol (33).

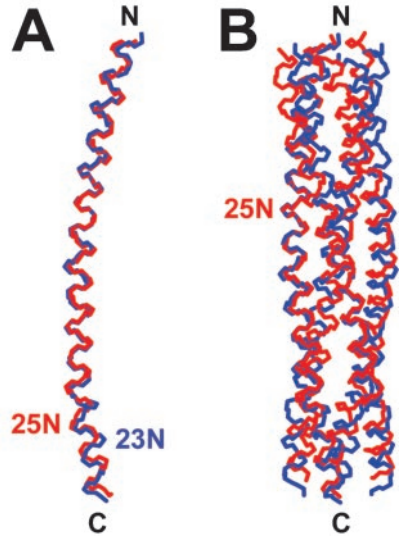

FIG. 6. **Superimposition of SNAP-23N with SNAP-25N.** *A*, backbone of SNAP-23N (*blue*) is superimposed with the backbone of SNAP-25N (*red*) from the neuronal heterotetrameric SNARE complex (Protein Data Bank accession number 1SFC) (7). The root mean square deviation is 1.1 Å with the greatest deviation in structure for the C-terminal 14 residues of SNAP-23N (residues 63–76). *B*, superimposition of the tetrameric complexes using SNAP-25N as the target (*red chain* labeled *25N*). This figure was prepared with the program MolMol (33).

veals a backbone root mean square deviation of only 1.1 Å in which greatest variability occurs over a small region at the C terminus (Fig. 6*A*). This structural difference may stem from an inherent difference between SNAP-23 and SNAP-25, the conformational lability of the SNAP-23N C-terminal region, or the fact that SNAP-23N in a homotetrameric complex is being compared with SNAP-25N in a heterotetrameric complex.

Hydrophobic intermolecular contacts are found in all SNARE complex structures. Interestingly, the packing of hydrophobic *a* and *d* residues (Fig. 1) to form a parallel four-helix bundle can be predicted from the SNAP-23N sequence using rules proposed by Harbury *et al.* (27). An enrichment of β-branched residues at the *d* position but not the *a* position favors coiled-coil tetramers, whereas the reverse pattern favors coiled-coil dimers. Each intermolecular layer of our structure has the same four hydrophobic side chains as a result of the 4-fold symmetry, whereas other SNARE complex structures have different hydrophobic side chains in each layer. The latter is also true for the syntaxin-1a homotetrameric structure, because the chains in this complex are antiparallel (26). Bulky hydrophobic side chains are accommodated by complementary smaller hydrophobic ones in each layer of these other SNARE complex structures (4). The SNAP-23N sequence lacks bulky hydrophobic side chains that would clash with one another as a result of parallel packing. Therefore, SNAP-23N may be unique among SNARE coiled-coil domains in its ability to form a parallel homotetrameric complex.

The SNAP-23N structure has buried glutamines in the 0 layer like other SNARE complexes (7, 24, 26). Buried polar residues at the center of coiled-coil complexes are thought to be important for orienting the direction of coiled-coil complexes (28, 29). The molecular arrangement of the 0 layer varies among SNARE complex structures. The three buried glutamines in the neuronal heterotetrameric complex structure are stabilized by hydrogen bond contacts between their carbonyl groups and the guanidinium side chain of an arginine from VAMP-2 (7). A network of water molecules coordinates the four buried glutamines in the SNAP-25N/syntaxin-1a tetrameric complex (24). The buried glutamines in the syntaxin-1a homotetramer hydrogen bond directly to each other as in our structure (26). However, in contrast to the SNAP-23N structure, the four glutamines in the syntaxin-1a structure are arranged in pairs on opposite sides of the complex due to the antiparallel topology of the helices. Therefore, the hydrogen bonding arrangement of the four buried glutamines in the SNAP-23N homotetramer is a new variant to the SNARE complex 0 layer (Fig. 5*B*).

Finally, the surface of the SNAP-23N structure is mostly acidic like other SNARE complexes (Fig. 4*C*) (7, 24, 26). It was speculated that SNARE regulatory molecules, NSF and SNAPs, have diverse recognition properties for different SNARE complexes by surface complementarity rather than for a specific sequence (30).

The biological significance of the homotetramer we observe is unclear. To date, homooligomerization of SNAP-23 has not been demonstrated *in vivo*. However, SNARE complex assembly is difficult to study in cells, and therefore purified SNARE proteins are used as a surrogate for this process (23, 31). What is the conformation of a v-SNARE or t-SNARE prior to vesicle fusion? One possibility is that SNAREs are disordered on membranes before interacting to form a membrane fusion complex. On the other hand, this seems unlikely given the growing data base of assembly intermediate structures. Furthermore, the high local concentrations of SNARE proteins on membranes should favor oligomerization. We propose that the SNAP-23N homotetramer and other assembly intermediates may represent low stability "storage forms." This could prevent proteolytic degradation of SNAREs yet allow rapid reorganization into high affinity heterotetrameric "fusion-active" forms. Future studies will be necessary to demonstrate SNARE complex intermediates within cells.

In summary, we have shown that SNAP-23N forms a heterotetrameric complex with other non-neuronal SNARE coiled-coil domains and, independently, self-associates to form a parallel homotetramer. The homotetrameric SNAP-23N structure has common and unique features compared with other reported SNARE complex structures and extends our understanding of SNARE coiled-coil complex diversity and SNAP-23 function.

Acknowledgments—We thank Amira Klip, Pietro De Camilli, and Richard Scheller for providing cDNA clones of human SNAP-23, rat VAMP-3, and rat syntaxin-4, respectively. We also thank Anand Saxena and Robert Sweet for help with x-ray data collection at beamline X-12C of the National Synchrotron Light Source of Brookhaven National Laboratories and Robert Flaumenhaft and Steven Blacklow for helpful discussions.

REFERENCES

1. Lin, R. C., and Scheller, R. H. (2000) *Annu. Rev. Cell Dev. Biol.* **16,** 19–49
2. Sollner, T., Whiteheart, S. W., Brunner, M., Erdjument-Bromage, H., Geromanos, S., Tempst, P., and Rothman, J. E. (1993) *Nature* **362,** 318–324
3. Sollner, T., Bennett, M. K., Whiteheart, S. W., Scheller, R. H., and Rothman, J. E. (1993) *Cell* **75,** 409–418
4. Fasshauer, D., Sutton, R. B., Brunger, A. T., and Jahn, R. (1998) *Proc. Natl. Acad. Sci. U. S. A.* **95,** 15781–15786
5. Chen, Y. A., and Scheller, R. H. (2001) *Nat. Rev. Mol. Cell. Biol.* **2,** 98–106
6. Poirier, M. A., Xiao, W., Macosko, J. C., Chan, C., Shin, Y. K., and Bennett, M. K. (1998) *Nat. Struct. Biol.* **5,** 765–769
7. Sutton, R. B., Fasshauer, D., Jahn, R., and Brunger, A. T. (1998) *Nature* **395,** 347–353
8. Antonin, W., Fasshauer, D., Becker, S., Jahn, R., and Schneider, T. R. (2002) *Nat. Struct. Biol.* **9,** 107–111
9. Ravichandran, V., Chawla, A., and Roche, P. A. (1996) *J. Biol. Chem.* **271,** 13300–13303
10. Wong, P. P., Daneman, N., Volchuk, A., Lassam, N., Wilson, M. C., Klip, A., and Trimble, W. S. (1997) *Biochem. Biophys. Res. Commun.* **230,** 64–68
11. Bennett, M. K., Garcia-Arraras, J. E., Elferink, L. A., Peterson, K., Fleming, A. M., Hazuka, C. D., and Scheller, R. H. (1993) *Cell* **74,** 863–873
12. McMahon, H. T., Ushkaryov, Y. A., Edelmann, L., Link, E., Binz, T., Niemann, H., Jahn, R., and Sudhof, T. C. (1993) *Nature* **364,** 346–349
13. Foster, L. J., Yeung, B., Mohtashami, M., Ross, K., Trimble, W. S., and Klip, A. (1998) *Biochemistry* **37,** 11089–11096
14. Yang, B., Gonzalez, L., Jr., Prekeris, R., Steegmaier, M., Advani, R. J., and Scheller, R. H. (1999) *J. Biol. Chem.* **274,** 5649–5653
15. Otwinowski, Z., and Minor, W. (1997) *Methods Enzymol.* **276,** 307–326
16. Jogl, G., Tao, X., Xu, Y., and Tong, L. (2001) *Acta Crystallogr. Sect. D Biol. Crystallogr.* **57,** 1127–1134
17. Terwilliger, T. C., and Berendzen, J. (1999) *Acta Crystallogr. Sect. D Biol. Crystallogr.* **55,** 849–861
18. Jones, T. A., Zou, J. Y., Cowan, S. W., and Kjeldgaard. (1991) *Acta Crystallogr Sect. A* **47,** 110–119
19. Brunger, A. T., Adams, P. D., Clore, G. M., DeLano, W. L., Gros, P., Grosse-Kunstleve, R. W., Jiang, J. S., Kuszewski, J., Nilges, M., Pannu, N. S., Read, R. J., Rice, L. M., Simonson, T., and Warren, G. L. (1998) *Acta Crystallogr. Sect. D Biol. Crystallogr.* **54,** 905–921
20. Bracher, A., Kadlec, J., Betz, H., and Weissenhorn, W. (2002) *J. Biol. Chem.* **277,** 26517–26523
21. Pinxteren, J. A., O'Sullivan, A. J., Larbi, K. Y., Tatham, P. E., and Gomperts, B. D. (2000) *Biochimie* (*Paris*) **82,** 385–393
22. Fasshauer, D., Eliason, W. K., Brunger, A. T., and Jahn, R. (1998) *Biochemistry* **37,** 10354–10362
23. Margittai, M., Fasshauer, D., Pabst, S., Jahn, R., and Langen, R. (2001) *J. Biol. Chem.* **276,** 13169–13177
24. Misura, K. M., Gonzalez, L. C., Jr., May, A. P., Scheller, R. H., and Weis, W. I. (2001) *J. Biol. Chem.* **276,** 41301–41309
25. Xiao, W., Poirier, M. A., Bennett, M. K., and Shin, Y. K. (2001) *Nat. Struct. Biol.* **8,** 308–311
26. Misura, K. M., Scheller, R. H., and Weis, W. I. (2001) *J. Biol. Chem.* **276,** 13273–13282
27. Harbury, P. B., Zhang, T., Kim, P. S., and Alber, T. (1993) *Science* **262,** 1401–1407
28. Akey, D. L., Malashkevich, V. N., and Kim, P. S. (2001) *Biochemistry* **40,** 6352–6360
29. Oakley, M. G., and Kim, P. S. (1998) *Biochemistry* **37,** 12603–12610
30. Brunger, A. T. (2001) *Curr. Opin. Struct. Biol.* **11,** 163–173
31. Fiebig, K. M., Rice, L. M., Pollock, E., and Brunger, A. T. (1999) *Nat. Struct. Biol.* **6,** 117–123
32. Sack, J. S. (1988) *J. Mol. Graph.* **6,** 244–245
33. Koradi, R., Billeter, M., and Wuthrich, K. (1996) *J. Mol. Graph.* **14,** 29–32, 51–55
34. Nicholls, A., Sharp, K. A., and Honig, B. (1991) *Proteins* **11,** 281–296

Homotetrameric Structure of the SNAP-23 N-terminal Coiled-coil Domain

Steven J. Freedman, Hyun Kyu Song, Yingwu Xu, Zhen-Yu J. Sun and Michael J. Eck

J. Biol. Chem. 2003, 278:13462-13467.
doi: 10.1074/jbc.M210483200 originally published online January 29, 2003
